Electronic Supplementary Information

Achieving near-Pt hydrogen production on defect nanocarbon via the synergy between carbon defects and heteroatoms

Hao Wu[a] and Yuting luan*[b]

[a] Key Laboratory of Functional Inorganic Material Chemistry (Ministry of Education of China), School of Chemistry and Materials Science, Heilongjiang University, 74# Xuefu Road, Nangang District, Harbin 150080, People's Republic of China;

[b] School of Food Engineering, Harbin University, 109# Zhongxing Avenue, Nangang District, Harbin 150080, People's Republic of China.

* Corresponding author E-mail: haowu@hlju.edu.cn.

Table of contents

1. Experimental Section

1.1 Reagents

Multi-walled carbon nanotube (CNT, purity > 95 %, 10-30 μm in length, 10-30 nm in diameter) was purchased from Chengdu Organic Chemicals Co., Ltd and, before use, CNT was acidified[S1] and soaked in 6.0 M HCl, which was renewed every five days, for at least a month in order to completely remove metal impurities. Carbon fiber (CF, purity > 99 %, 10-20 μm in length, 150-200 nm in diameter) was received from Showa Denko and, before use, CF was pre-treated using the same procedure as used for the CNT. Flake graphite was obtained from Nanjing XFNANO Materials Tech Co., Ltd and graphene oxide (GO) was prepared using a modified Hummers' method reported in the literature (the mass ratio of graphite and $KMnO_4$ was 1 : 3).[S2] Melamine (99.5 % purity) and phosphoric acid (85 wt.%) were purchased from Tianjin Guangfu Fine Chemical Research Institute and Tianli Chemical Reagent Co., Ltd., respectively. Commercial Pt/C (20 % Pt on Vulcan XC-72) and Nafion 117 solution (5 % (w/w) in low aliphatic alcohols and water) were obtained from Johnson Matthey Fuel Cells and Sigma-Aldrich LLC, respectively. Ultra-pure water (18.2 Ωm) used throughout all experiments was received from a Milli-Q Water System (Millipore Corp., Bedford, MA, USA). All the other reagents were of analytical grade and used without further purification in this work.

References:

S1. H. Wu, Z. M. Chen, J. L. Zhang, F. Wu, C. Y. He, B. Wang, Y. Q. Wu and Z. Y. Ren, *J. Mater. Chem. A.*, 2016, 4, 1096-1104.

S2. J. T. Zhang, L. T. Qu, G. Q. Shi, J. Y. Liu, J. F. Chen and L. M. Dai, *Angew. Chem. Int. Ed.*, 2016, 55, 2230-2234.

1.2 Preparation of CNT-NP

CNT-NP was prepared by the pyrolysis of H-bonding driven melamine-phosphoric acid/CNT (CNT@MP) assemblies. Briefly, 40 mg of CNT was sonicated in 100 mL of ultra-pure water at room temperature for 2 h. Subsequently, a certain amount of melamine and phosphoric acid were added under vigorous stirring. Next, the mixture was continuously stirred for 2 h in water bath at 90 ºC. After natural cooling to room temperature, the product was filtered and washed with ultra-pure water, methanol, and ether until the filtrate was colorless, then dried in a vacuum oven for 2 h at 80 ºC, affording the CNT@MP assemblies as brownish black powders. Finally,

the assemblies were calcined at 900 ºC for 2 h in N_2 atmosphere with a ramp rate of 5 ºC min^{-1}. After the furnace was naturally cooled down to room temperature under a flowing N_2 atmosphere, the desired CNT-NP was obtained. The detailed dosages of melamine and phosphoric acid in the synthesis of CNT-NP with different proportion and content of N and P were listed in **Table S7**.

As a control, N doped CNT (CNT-N) was prepared by thermal-treating the mixture of CNT (40 mg) and melamine (100 mg) at 900 ºC for 2 h in N_2 atmosphere with a ramp rate of 5 ºC min^{-1}. P doped CNT (CNT-P) was prepared using the same procedure as used for CNT-N except that melamine was replaced with triphenylphosphine (400 mg). N, P co-doped carbon fiber (CF-NP) and N, P co-doped graphene (G-NP) were prepared using the same procedure as used for CNT-NP, and the detailed dosages of melamine and phosphoric acid were listed in **Table S8**.

1.3 Preparation of CNT-VP

CNT-VP was obtained from CNT-NP by a tenderly electrochemical etching. Briefly, 1 mg of CNT-NP was dispersed in the 0.2 mL ethanol/5 wt.% Nafion (200 μL/10 μL) solution for at least 20 min of ultrasonication. A 20 μL amount of this catalyst ink was dropped onto a well-polished glassy carbon electrode (GCE) surface (4 mm in diameter). Then, the GCE was undergone an electrochemical etching by a continuous cyclic voltammetry (CV) from – 0.1 and – 1.0 V (vs. RHE) with a saturated calomel electrode (SCE) as the reference electrode and a graphite rod as the counter electrode in 0.5 M H_2SO_4 (scan rate: 2 mV s^{-1}). After 1000 cycles, the product was separated from GCE surface, washed with ultra-pure water and methanol, and then lyophilized, affording CNT-VP as black powders.

As a control, vacancy doped CNT (CNT-V) was prepared using the same procedure as used for CNT-VP except that CNT-NP was replaced with CNT-N. CF-VP and G-VP were prepared using the same procedure as used for CNT-VP except that CNT-NP was replaced with CF-NP or G-NP.

1.4 Characterization

Transmission electron microscopy (TEM) images and the scanning TEM-energy-dispersive X-ray spectroscopy (STEM-EDS) mapping were acquired on a Tecnai G2 F20 electron microscope (FEI, USA) with an acceleration voltage of 200 kV. X-ray diffraction (XRD)

patterns were performed on a 40 kV D/max-IIIB diffractometer (Rigaku) by Cu K_α radiation (λ = 1.5406 Å). Raman spectra was obtained on a HR800 UV spectrometer (Jobin Yvon) excited by a laser of 457.9 nm. The N and P K-edge soft X-ray absorption near-edge structure (SXANES) analyses were implemented on 4B9B and 4B7A beamline at Beijing Synchrotron Radiation Facility (BSRF, China). The energy resolutions in 4B9B and 4B7A beamline were 0.20 and 0.30 eV, respectively. SXANES spectra were recorded in fluorescence yield (FY) mode and the storage ring was operated at 2.5 GeV with a beam current of approximately 250 mA. X-ray photoelectron spectroscopy (XPS) was collected using a AXIS Ultra spectrometer (Kratos) equipped with a delay line detector in ultrahigh vacuum. The binding energies in the XPS analysis were internally standardized with respect to C 1s (284.8 eV). Inductively coupled plasma-atomic emission spectroscopy (ICP-AES) analysis was collected on Optima 7000 DV (Perkin-Elmer). Samples for ICP-AES were prepared by ashing 10 mg of sample in muffle furnace (air atmosphere) at 800 °C for 2 h, and then leached out with HCl (10 wt % in water) and volume to 5 mL. ^{1}H nuclear magnetic resonance (^{1}H-NMR) was determined on an ultrashield400 (Bruker). The conductivity of the samples was measured using a RM3000+ 4-point probe instrument (Jandel Engineering Ltd.) by repeating the test in at least 10 different positions.

1.5 Electrochemical measurements

The electrochemical measurements were taken on the CHI 760D electrochemical workstation equipped with a three-electrode system (CH instruments, Shanghai, China) in 0.5 M H_2SO_4 aqueous solution at room temperature (25 ± 1 ºC). A studied catalyst modified glassy carbon electrode (GCE) served as the working electrode, while graphite rod and saturated calomel electrode were used as the auxiliary and reference electrodes, respectively. All the potentials involved in this work were normalized to the reversible hydrogen electrode (RHE). The electrolyte was constantly bubbled with H_2 gas (99.999 % purity) to avoiding the effects of dissolved oxygen and maintaining a constant RHE potential. For preparing working electrode, 1 mg of catalyst mixed with 10 μL of 5 wt.% Nafion was ultrasonically dispersed in 0.2 mL of ethanol until homogenous catalyst ink was obtained. Than, 20 μL of this catalyst ink was drop casted on the well-polished GCE surface evenly (the catalyst loading ~ 0.378 mg cm^{-2}) and allowed to dry under an infrared lamp. Linear sweep voltammetry (LSV) was measured for the

polarization curves (scan rate: 2 mV s^{-1}) and all the polarization curves were recorded with 100 % *iR* compensation. The Tafel slope is obtained from Tafel equation as follows: $\eta = b \times log(j/j_0)$, where η is the overpotential, b is the Tafel slope, j is the current density, and j_0 is the exchange current density, respectively. The electrochemical doublelayer capacitance (C_{dl}) was determined by CV method in a N_2-saturated 0.5 M H_2SO_4 aqueous solution and a non-Faradaic region at different scan rates of 40, 60, 80, 100, 120, 140, 160, 180 $mV \cdot s^{-1}$. Electrochemical impedance spectra (EIS) were recorded at open circuit potential with an amplitude of 5 mV over a frequency range from 0.01 to 100 kHz. The Faradic efficiency of HER catalystsis defined as the ratio of the amount of experimentally determined H_2 to that of the theoretically expected H_2 from the reaction. Accordingly, the H_2 evolved from the reaction was measured by gas chromatography (GC2002, Shanghai, China) with CH_4 as internal standard and N_2 as a carrier gas for quantitative analysis.

1.6 Determination of ammonia

Concentration of produced ammonia was determined by the indophenol blue method.[S3] In detail, 2 mL of 1 M NaOH solution containing salicylic acid (5 wt%) and sodium citrate (5 wt%) was added into 2 mL of the electrolyte after electrochemical etching, followed by addition of 1 mL of 0.05 M NaClO and 0.2 mL of $C_5FeN_6Na_2O$ (1 wt%). The absorption spectrum was measured using an UV-vis spectrophotometer. The concentration of indophenol blue was determined using the absorbance at a wavelength of 655 nm. The concentration-absorbance curve was calibrated using standard ammonia chloride solution with a serious of concentrations.

References:

S3. Z. G. Geng, Y. Liu, X. D. Kong, P. Li, K. Li, Z. Y. Liu, J. J. Du, M. Shu, R. Si and J. Zeng, *Adv. Mater.*, 2018, 30, 1803498.

1.7 TOF calculations

The TOFs of CNT-NP and CNT-VP in 0.5 M H_2SO_4 for HER is calculated by the equation:

$$TOF = \frac{Total\ number\ of\ hydrogen\ turnover/geometric\ area\ (cm^2)}{Number\ of\ active\ sites/geometric\ area\ (cm^2)}$$

Total number of hydrogen turnover[S4,S5]

$$= (j\ mA\ cm^{-2})\left(\frac{1\ C\ s^{-1}}{10^3\ mA}\right)\left(\frac{1\ mol\ e^-}{96485.3\ C}\right)\left(\frac{1\ mol\ H_2}{2\ mol\ e^-}\right)\left(\frac{6.022\ \times 10^{23}\ molecules\ H_2}{1\ mol\ H_2}\right) = per\ mA\ cm^{-2}$$

The number of active synergy sites is assumed to be equal to the number of N and all of these sites are accessible to the electrolyte. The real number of active and accessible sites should be considerably lower than the calculated value and the content of N is revealed by the XPS measurements. Accordingly, number of active sites

$$= \left(W_N \times \frac{1\ mmol}{14.004\ mg} \right) \times 0.378\ mg\ cm^{-2} \times 6.022 \times 10^{20}\ sites\ mmol^{-1}$$

Where W_N is the mass content of N.

References:

S4. H. W. Liang, S. Bruller, R. H. Dong, J. Zhang, X. L. Feng and K. Mullen, *Nat. Commun.*, 2015, 6, 7992.

S5. J. N. Tiwari, S. Sultan, C. W. Myung, T. Yoon, N. N. Li, M. R. Ha, A. M. Harzandi, H. J. Park, D. Y. Kim, S. S. Chandrasekaran, W. G. Lee, V. Vij, H. J. Kang, T. J. Shin, H. S. Shin, G. Lee, Z. Lee and K. S. Kim, *Nat. Energy*, 2018, 3, 773-782.

1.8 Calculation methods

DFT calculations were performed by using the CASTEP code.[S6,S7] The form of computing was delineated by the Perdew-Burke-Ernzerh (PBE) functional of the generalized gradient approximation (GGA). The ion-electron interaction was modelled by the frozen core all-electron projector augmented wave pseudopotentials. The electron wave functions were expanded by using a plane wave basis set with a cutoff energy of 400 eV. The structure of model was fully optimized by taking 0.01 eV $Å^{-1}$ as the convergence threshold. The density of states (DOS) was computed by using a 7 × 6 × 1 *k*-point mesh. The Gibbs free-energy of hydrogen adsorption (ΔG_{H^*}) at T = 298.15 K was obtained as $\Delta G_{H^*} = \Delta E_{H^*} + \Delta E_{ZPE} - T\Delta S_H$,[S8] where ΔE_{H^*} is the hydrogen absorption energy, ΔE_{ZPE} is the difference in zero point energy between the adsorbed hydrogen and hydrogen in the gas phase and ΔS_H is the entropy difference between the adsorbed state and the gas phase. Given that the vibrational entropy of hydrogen on the adsorbed state is extremely small,[S9] the formula for ΔG_{H^*} can also be simplified as $\Delta G_{H^*} = \Delta E_{H^*} + 0.24$ eV. And ΔE_{H^*} can be defined as $\Delta E_{H^*} = (1/n)(\Delta E_{M+nH^*} - \Delta E_M) - 0.5E_{H2}$, where ΔE_{M+nH^*} is the total energies of the doped graphene with *n* adsorbed H atoms on the surface, ΔE_M is the total energy of the doped graphene and E_{H2} is the energy of a H_2 molecule.

References:

S6. Y. S. Wu, X. J. Liu, D. D. Han, X. Y. Song, L. Shi, Y. Song, S. W. Niu, Y. F. Xie, J. Y.

Cai, S. Y. Wu, J. Kang, J. B. Zhou, Z. Y. Chen, X. S. Zheng, X. H. Xiao and G. M. Wang, *Nat. Commun.*, 2018, 9, 1425.

S7. J. Q. Zhu, Z. Y. Ren, S. C. Du, Y. Xie, J. Wu, H. Y. Meng, Y. Z. Xue and H. G. Fu, *Nano Res.*, 2017, 10, 1819-1831.

S8. Y. Zheng, Y. Jiao, Y. Zhu, L. H. Li, Y. Han, Y. Chen, A. Du, M. Jaroniec and S. Z. Qiao, *Nat. Commun.*, 2014, 5, 3783.

S9. Y. Ito, W. T. Cong, T. Fujita, Z. Tang and M. W. Chen, *Angew. Chem., Int. Ed.*, 2015, 54, 2131-2136.

2. Supplementary Figures

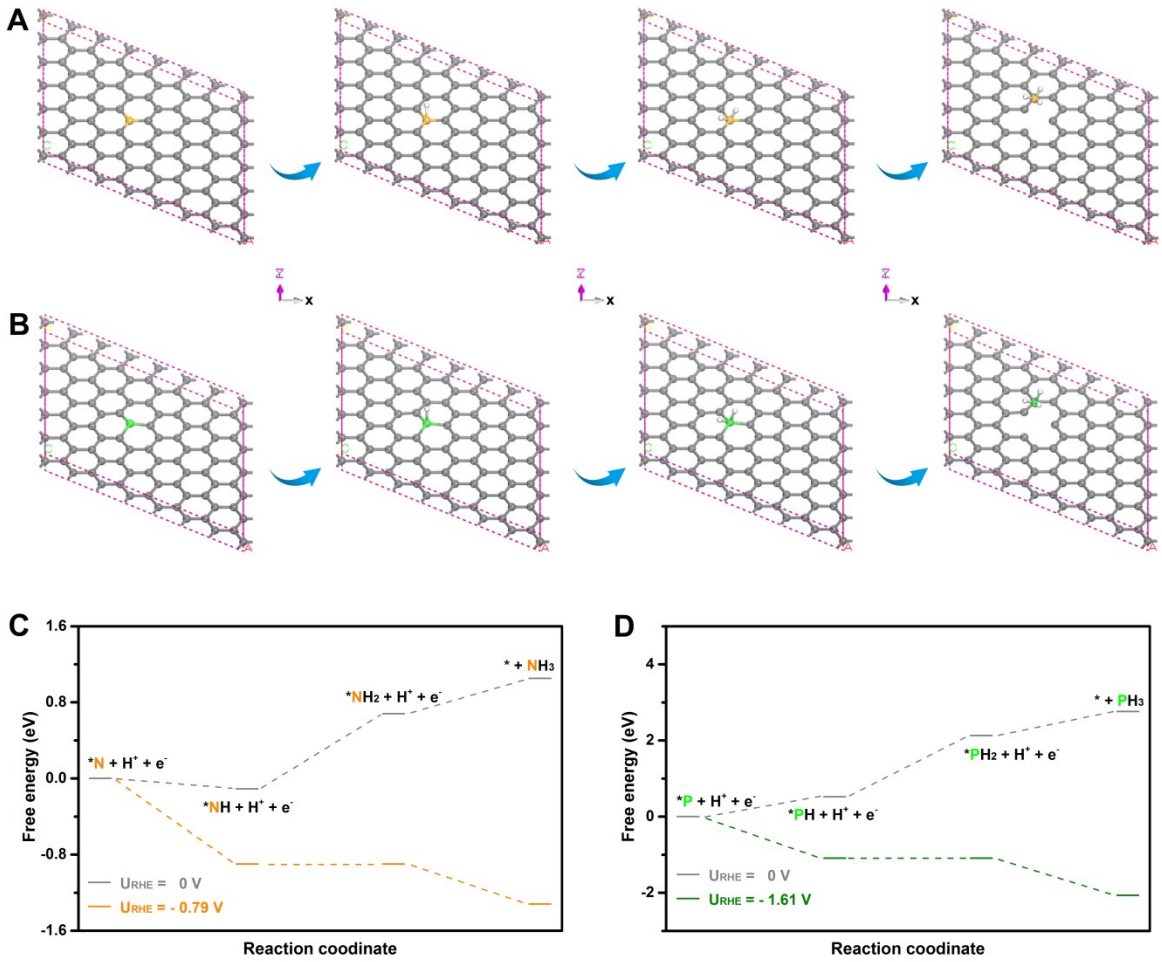

Fig. S1. (A and B) The optimized adsorption geometries corresponding to the proton–electron transfer steps in (C) and (D). The grey, orange, green and white balls respectively represent C, N, P and H atoms, and the unit cells of various models are indicated by purple dashed line. (C and D) The free energy diagram for the removal of N atom from N doped carbon (C) or P atom from P doped carbon (D). The * denotes a vacancy and the * prefix indicates that a species occupies a vacancy.

Fig. S1 show that the theoretical potential required to remove the N atom from N doped carbon (-0.79 V) under acidic conditions is significantly lower than that required to remove the P atom from P doped carbon (-1.61 V). This indicates that the N atom in the N, P co-doped carbon may be preferentially electrochemically etched away.

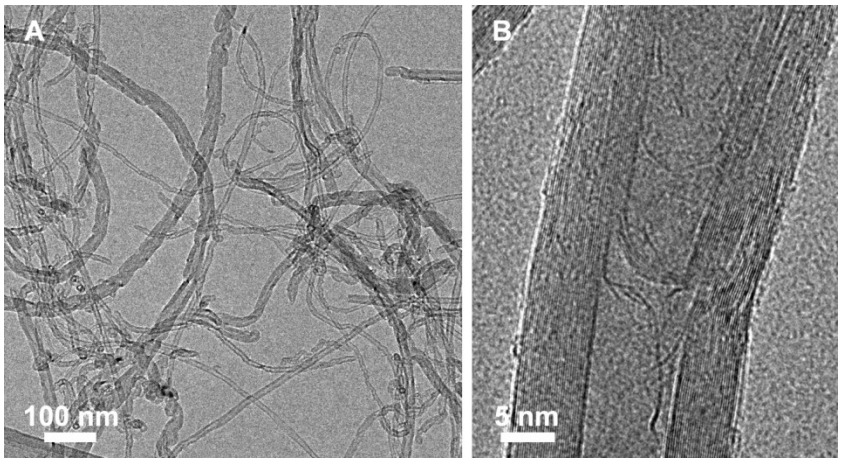

Fig. S2. TEM (A) and HRTEM (B) images of CNT.

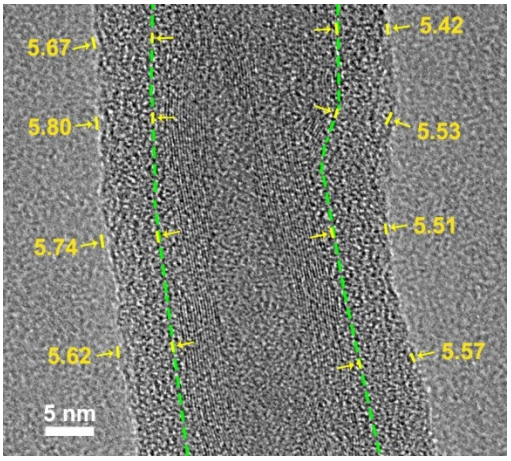

Fig. S3. HRTEM image of CNT@MP.

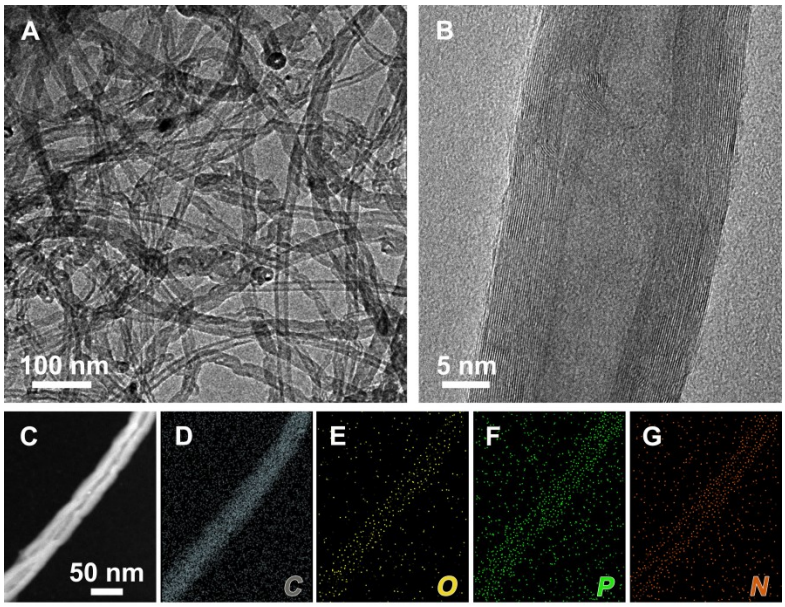

Fig. S4. TEM image (A), HRTEM image (B) and STEM-EDS mapping (C-G) of CNT-NP.

Fig. S5. The distribution of N on the surface of CNT-VP obtained from STEM-EDS mapping.

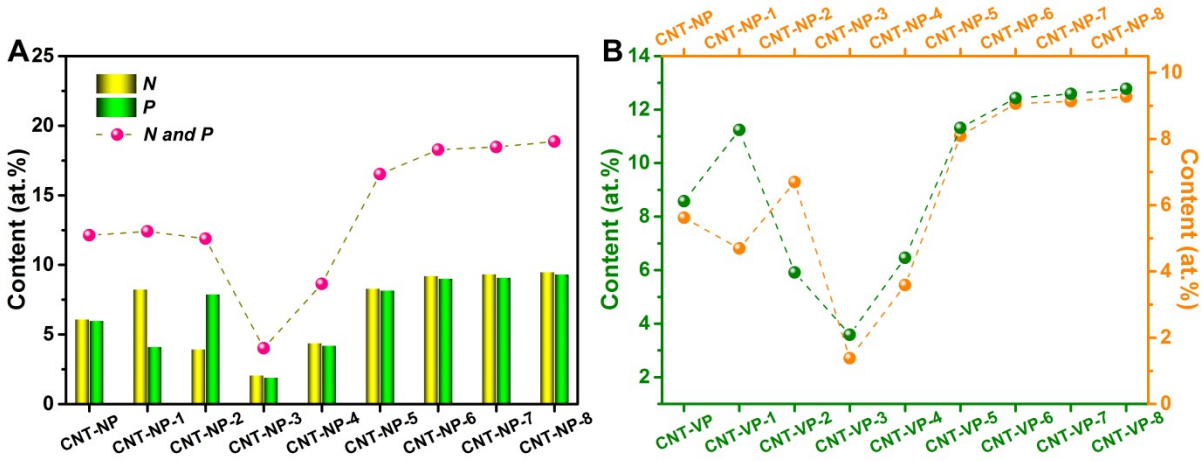

Fig. S6. The content of heteroatoms in CNT-NP (A), the content of P in CNT-VP and the content of N in CNT-NP (B) obtained from XPS analysis.

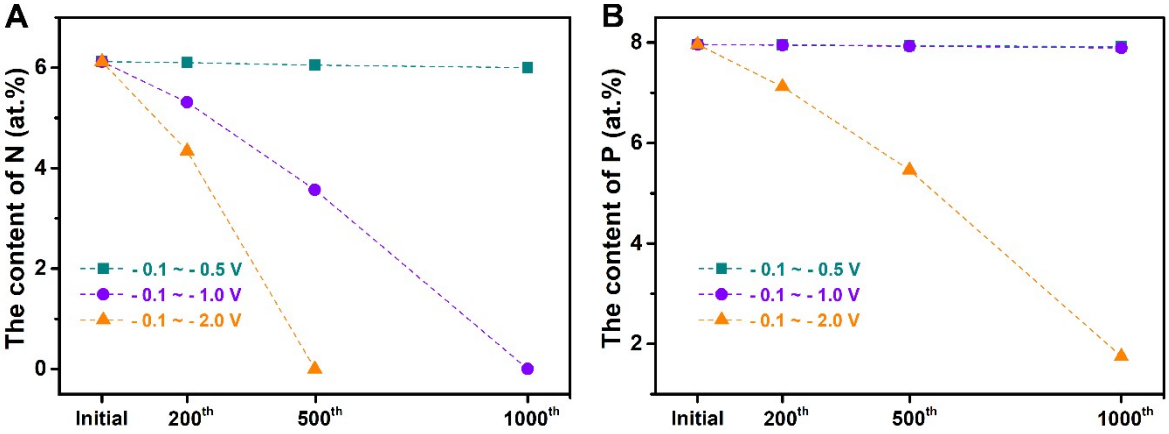

Fig. S7. The content of N in CNT-NP (A) and the content of P in CNT-VP (B) with different CV cycles and potential range (vs. RHE) in 0.5 M H_2SO_4 at the scan rate of 2 mV s^{-1}. These results were obtained from XPS analysis.

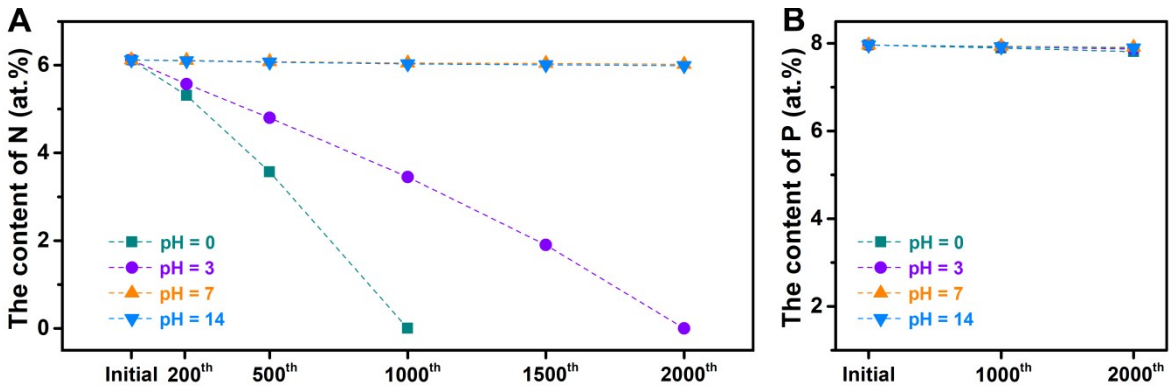

Fig. S8. The content of N in CNT-NP (A) and the content of P in CNT-VP (B) with different CV cycles between –0.1 and –1.0 V (vs. RHE) in solutions with different pH at the scan rate of 2 mV s^{-1}. These results were obtained from XPS analysis.

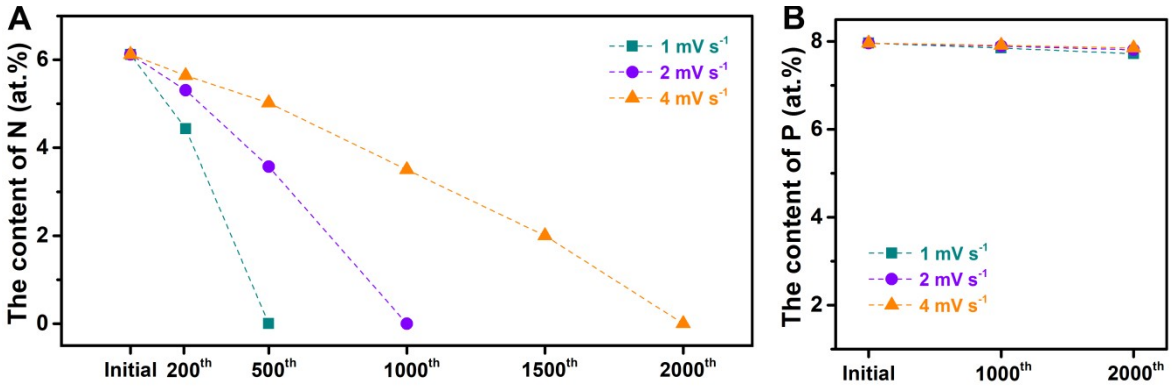

Fig. S9. The content of N in CNT-NP (A) and the content of P in CNT-VP (B) with different CV cycles between –0.1 and –1.0 V (vs. RHE) in 0.5 M H_2SO_4 at the scan rate of 1, 2 and 4 mV s^{-1}, respectively. These results were obtained from XPS analysis.

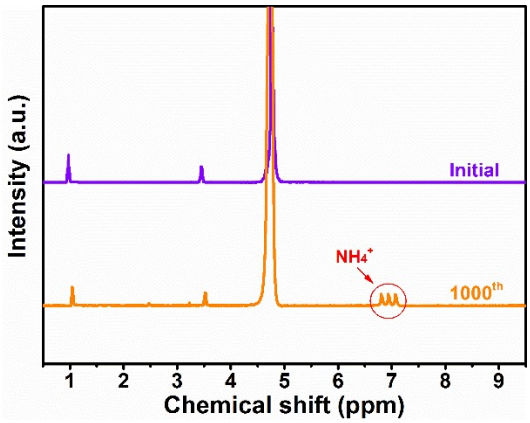

Fig. S10. ^{1}H-NMR of electrolyte in D_2O for CNT-NP initially and after 1000 cycles.

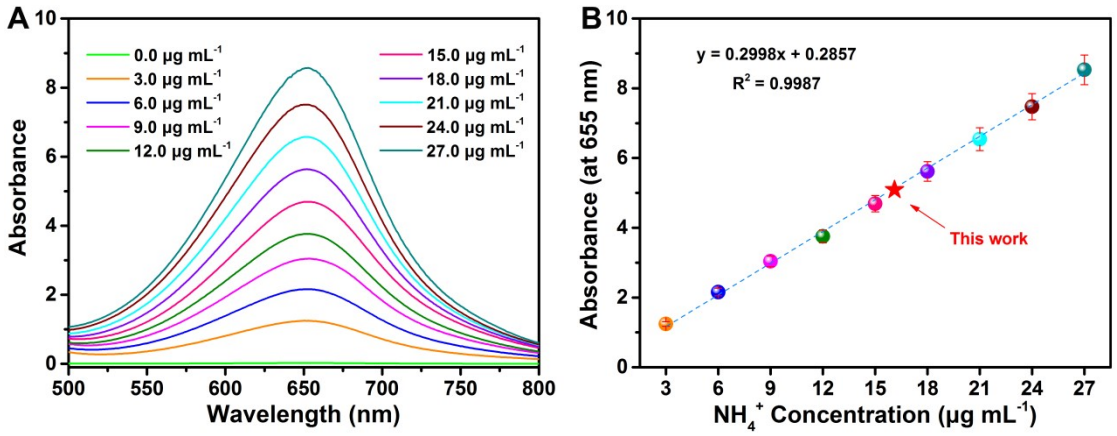

Fig. S11. UV-vis curves (A) and concentration-absorbance curve of NH_4^+ ions solution with a series of standard concentration (B). The absorbance at 655 nm was measured by UV-vis spectrophotometer. The standard curve showed good linear relation of absorbance with NH_4^+ ion concentration ($y = 0.2998x + 0.2857$, $R^2 = 0.9987$).

As shown in ***Fig. S11***, the indophenol blue method can be used to determine the content of NH_4^+ in the post-etching electrolyte. When 10 mg of CNT-NP is electrochemically etched, the content of NH_4^+ in 50 mL of electrolyte is found to be about 16.11 μg mL^{-1}.

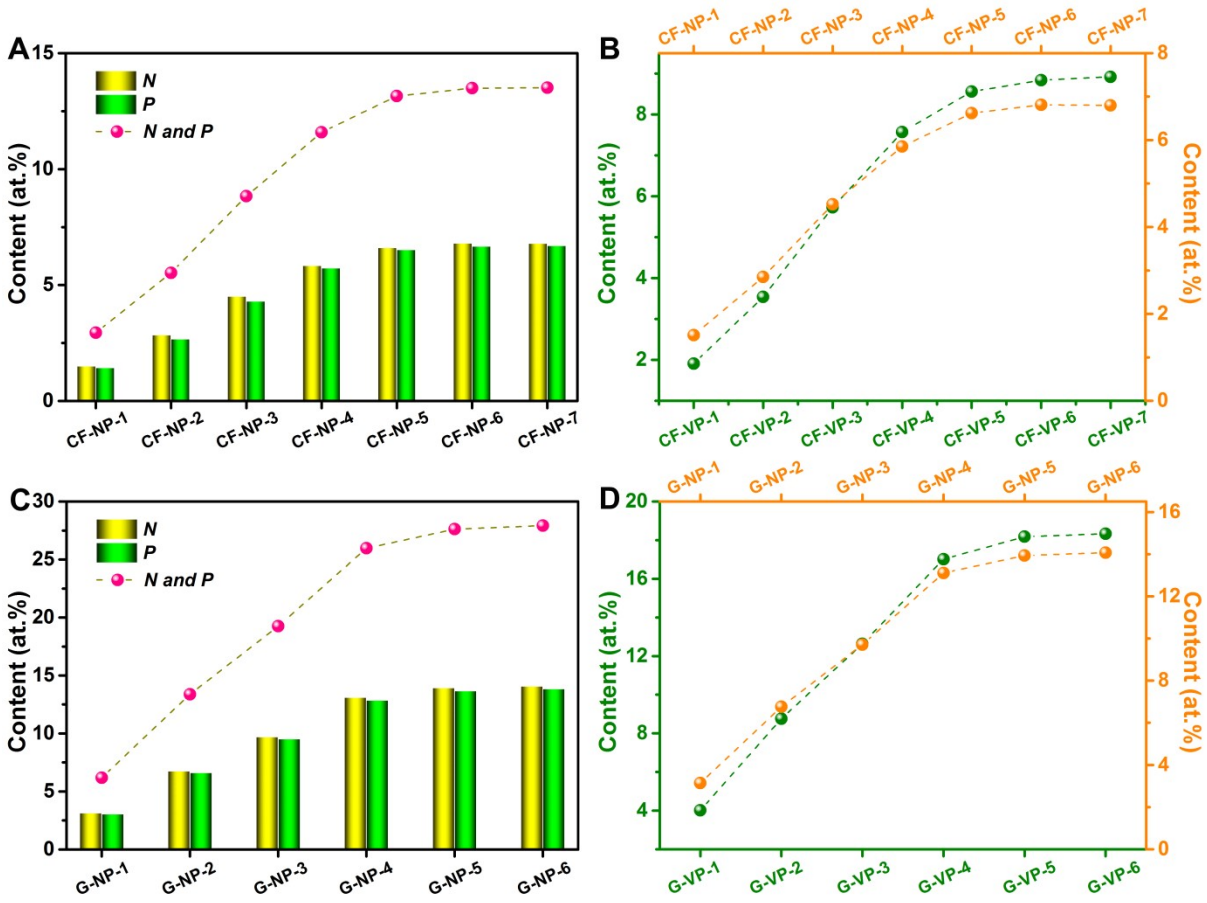

Fig. S12. (A) The content of heteroatoms in CF-NP. (B) the content of P in CF-VP and the content of N in CF-NP. (C) The content of heteroatoms in G-NP. (D) the content of P in G-VP and the content of N in G-NP.

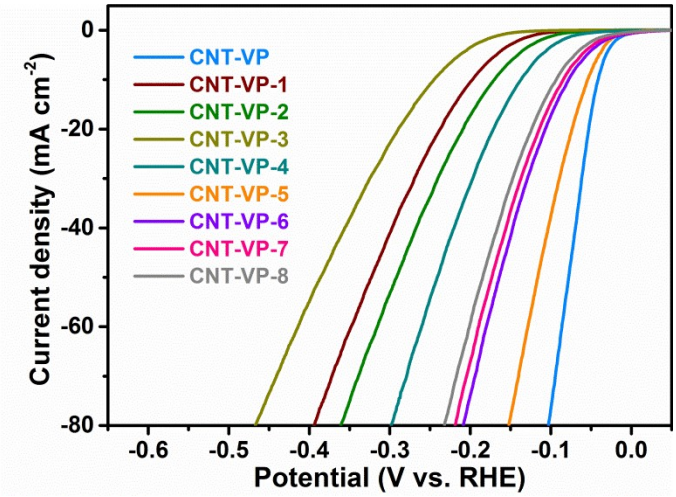

Fig. S13. *iR*-compensated HER polarization curves of the various CNT-VP catalysts in 0.5 M H_2SO_4.

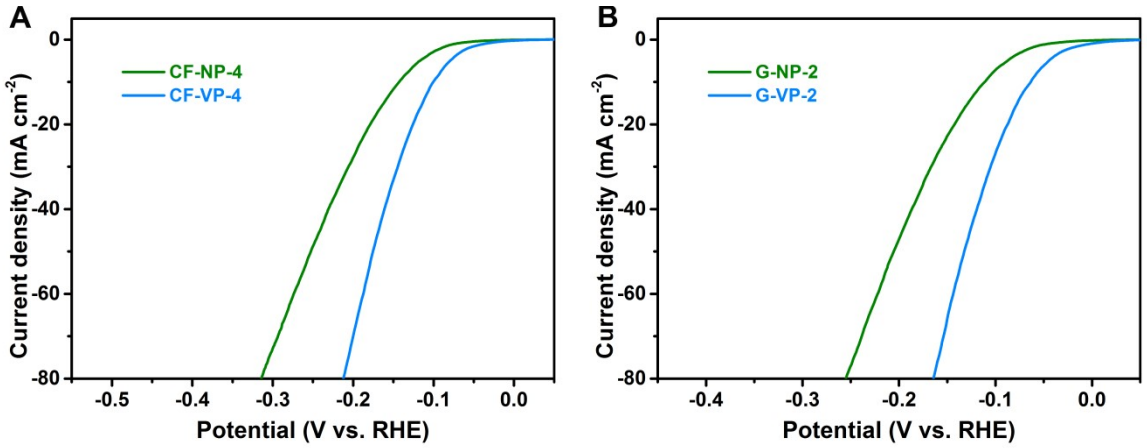

Fig. S14. *iR*-compensated HER polarization curves of CF-NP-4 and CF-VP-4 (A) and G-NP-2 and G-VP-2 (B) in 0.5 M H_2SO_4.

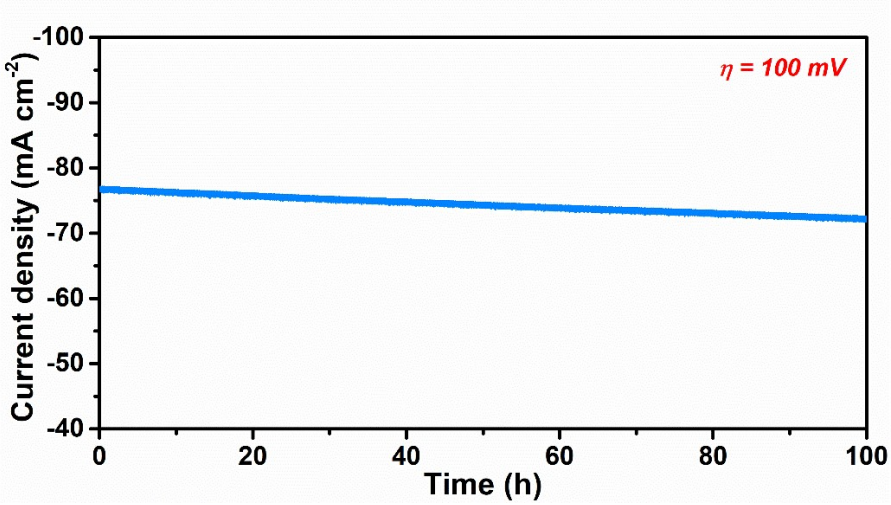

Fig. S15. *iR*-compensated time dependence of the current density for 100 h (η = 100 mV) of CNT-VP in 0.5 M H_2SO_4.

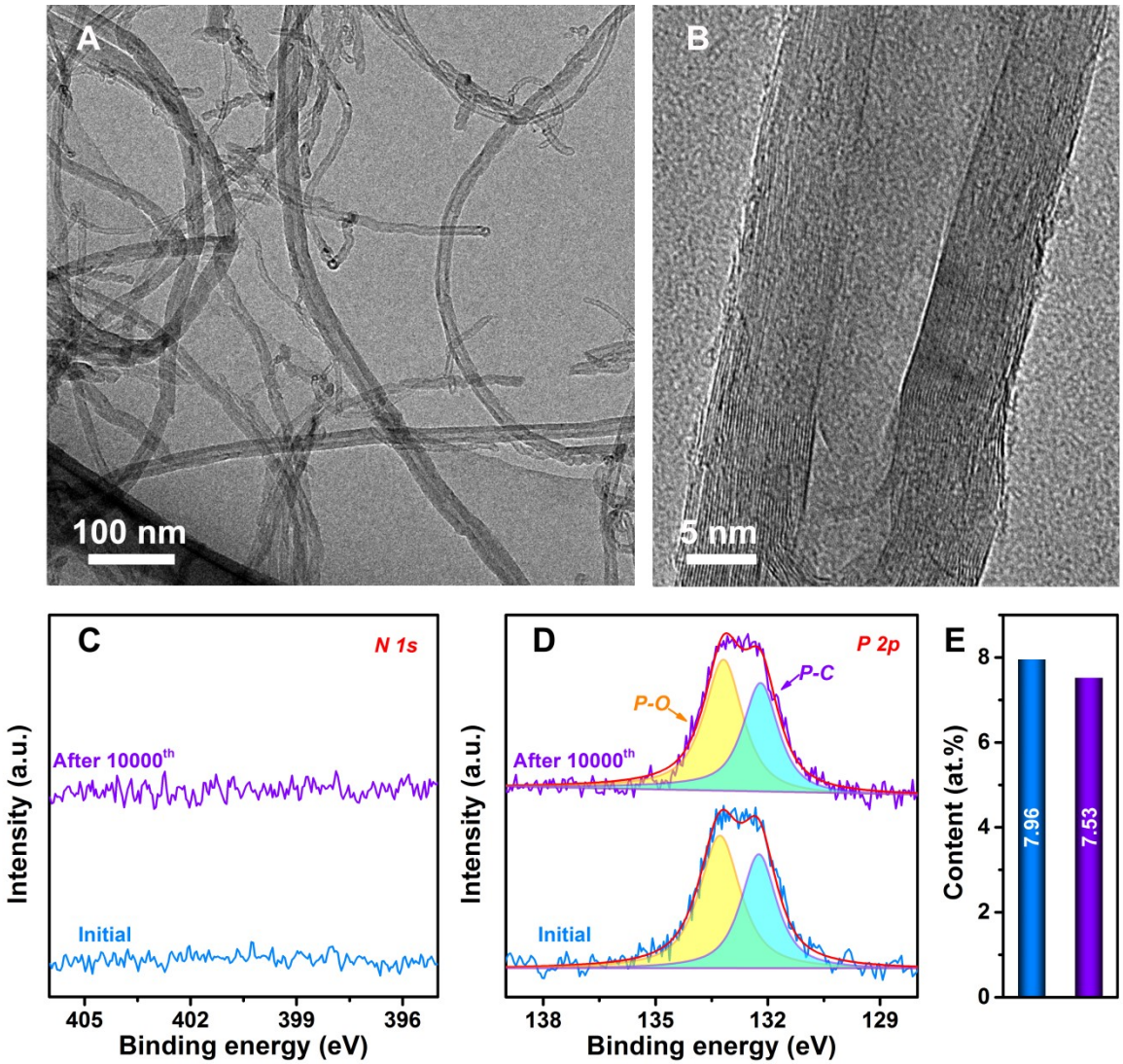

Fig. S16. (A and B) TEM (A) and HRTEM (B) images of CNT-VP after 10000 CV cycles. (C-E) The high-resolution N 1s XPS spectra (C), high-resolution P 2p XPS spectra (D) and the corresponding P atomic percentages (E) of CNT-VP initially and after 10000 CV cycles.

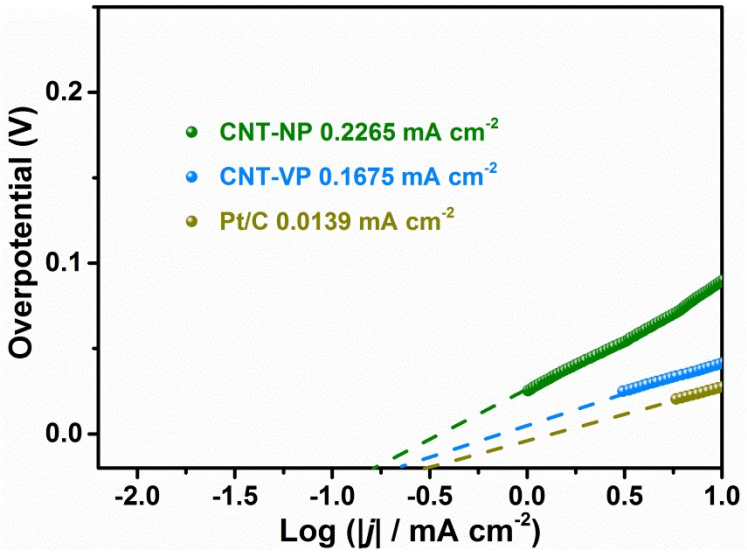

Fig. S17. The measured j_0 of CNT-NP, CNT-VP and Pt/C by using an extrapolation method.

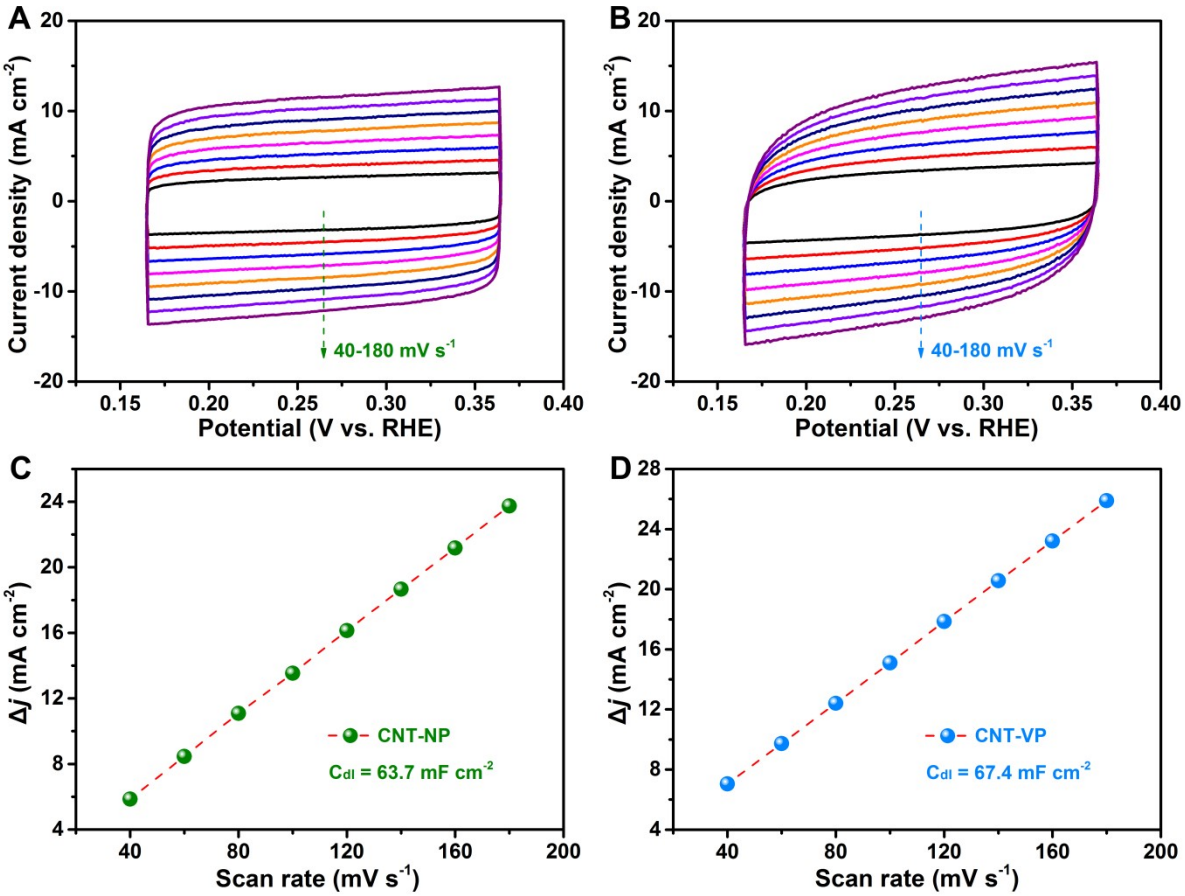

Fig. S18. (A and B) CVs for CNT-NP (A) and CNT-VP (B) at different scan rate from 40 to 180 mV s^{-1}. (C and D) The differences in current density (Δj) at 0.265 V (vs. RHE) as a function of scan rate for CNT-NP (C) and CNT-VP (D).

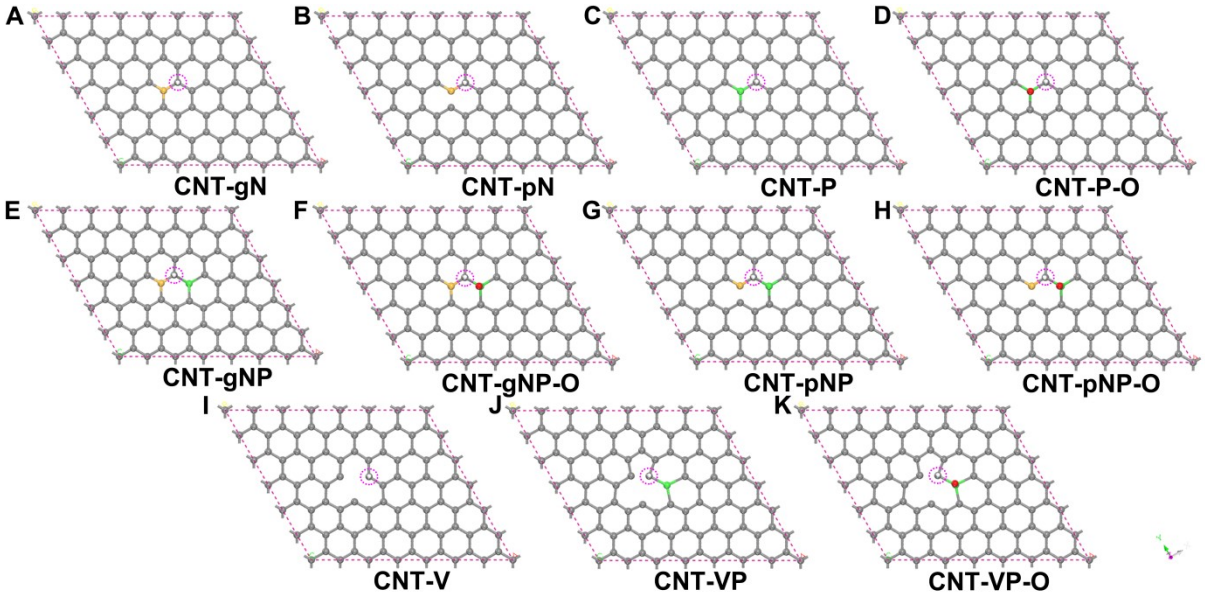

Fig. S19. A variety of optimized models used to simulate the structure of CNT-VP and reference samples, in which the most active of hydrogen adsorption sites are indicated by a pink dot circle. The grey, orange, red, green and white balls respectively represent C, N, O, P and H atoms, and the unit cells of various models are indicated by purple dashed line.

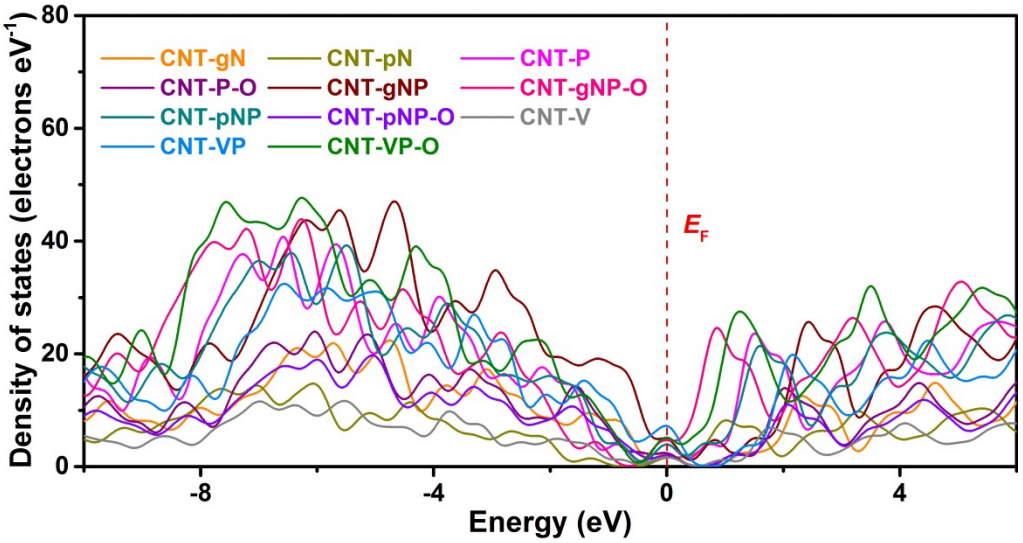

Fig. S20. The DOS plots of CNT-VP and reference models.

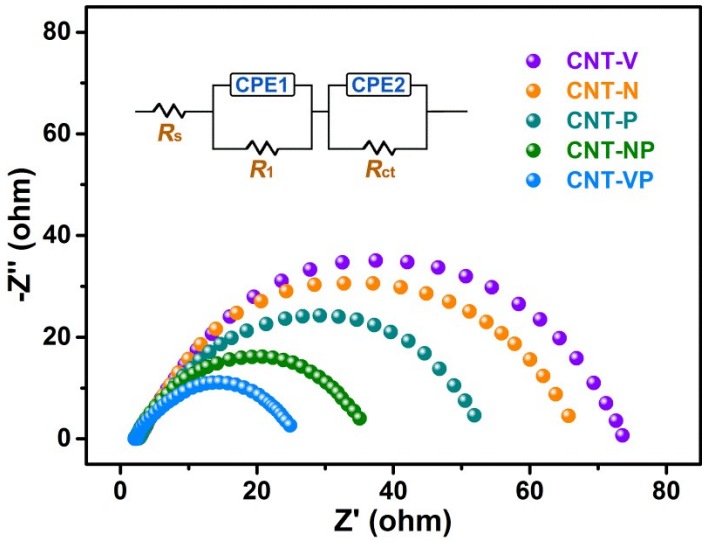

Fig. S21. Nyquist plots of CNT-V, CNT-N, CNT-P, CNT-NP and CNT-VP, the inset is the equivalent circuit model applied to fit the Nyquist plots, where R_s is the electrolyte resistance, R_1 relates to the interfacial resistance resulting from the electron transport between the catalyst and the GCE, R_{ct} is the charge-transfer resistance and CPE1 and CPE2 represent the double layer capacitance.

2. Supplementary Tables

Table S1. The typical Raman bands of MP.[S10,S11]

Raman shift (cm^{-1})	Assignment
983	Ring breathing mode of triazine ring
918	PO_4 stretching
690	Ring breathing mode and an in-plane deformation of triazine ring
572	PO_4 bending in HPO_4^{2-} group
382	PO_4 bending in $H_2PO_4^{2-}$ group

References:

S10. I. Liascukiene, M. Ben Salah, R. Sabot, P. Refait, L. Dhouibi, C. Methivier, J. Landoulsi and M. Jeannin, *Appl. Surf. Sci.*, 2018, 434, 561-572.

S11. J. M. Li, Y. Yang and D. Qin, *J. Mater. Chem. C*, 2014, 2, 9934-9940.

Table S2. The elemental composition of various CNT-NP and CNT-VP catalysts obtained from XPS analysis.

Samples	XPS analysis (at.%)				Samples	XPS analysis (at.%)			
	C	O	N	P		C	O	N	P
CNT-NP	84.66	3.21	6.12	6.01	**CNT-VP**	86.86	5.18	---	7.96
CNT-NP-1	85.37	2.22	8.27	4.14	**CNT-VP-1**	88.05	5.14	---	6.81
CNT-NP-2	83.71	4.41	3.97	7.91	**CNT-VP-2**	84.92	5.79	---	9.29
CNT-NP-3	94.85	1.13	2.09	1.93	**CNT-VP-3**	95.44	1.85	---	2.71
CNT-NP-4	89.39	1.97	4.41	4.23	**CNT-VP-4**	91.24	3.32	---	5.44
CNT-NP-5	79.33	4.15	8.33	8.19	**CNT-VP-5**	82.13	6.85	---	11.02
CNT-NP-6	77.10	4.63	9.23	9.04	**CNT-VP-6**	79.97	7.81	---	12.22
CNT-NP-7	77.01	4.52	9.36	9.11	**CNT-VP-7**	79.79	7.90	---	12.31
CNT-NP-8	76.36	4.78	9.51	9.35	**CNT-VP-8**	79.35	8.16	---	12.49

Notes: the content of N in various CNT-VP catalysts exceeds the detection limits of the machine (Kratos AXIS Ultra spectrometer).

***Table S3*.** The ICP-AES results of various CNT-VP catalysts.

Samples	Fe (wt.%)	Co (wt.%)	Ni (wt.%)	Pt (wt.%)
CNT-VP	<0.0010	<0.0010	<0.0010	<0.0010
CNT-VP-1	<0.0010	<0.0010	<0.0010	<0.0010
CNT-VP-2	<0.0010	<0.0010	<0.0010	<0.0010
CNT-VP-3	<0.0010	<0.0010	<0.0010	<0.0010
CNT-VP-4	<0.0010	<0.0010	<0.0010	<0.0010
CNT-VP-5	<0.0010	<0.0010	<0.0010	<0.0010
CNT-VP-6	<0.0010	<0.0010	<0.0010	<0.0010
CNT-VP-7	<0.0010	<0.0010	<0.0010	<0.0010
CNT-VP-8	<0.0010	<0.0010	<0.0010	<0.0010

Notes: the content of Fe, Co, Ni and Pt exceeds the detection limits of the machine (Perkin-Elmer Optima 7000 DV).

Table S4. The elemental composition of various CF-NP, CF-VP, G-NP and G-VP catalysts obtained from XPS analysis.

Samples	XPS analysis (at.%)				Samples	XPS analysis (at.%)			
	C	O	N	P		C	O	N	P
CF-NP-1	96.16	0.89	1.51	1.44	**CF-VP-1**	96.63	1.46	---	1.91
CF-NP-2	92.88	1.59	2.85	2.68	**CF-VP-2**	93.73	2.73	---	3.54
CF-NP-3	88.89	2.28	4.52	4.31	**CF-VP-3**	90.34	3.93	---	5.73
CF-NP-4	85.40	3.01	5.85	5.74	**CF-VP-4**	87.29	5.14	---	7.57
CF-NP-5	83.38	3.47	6.62	6.53	**CF-VP-5**	85.59	5.85	---	8.56
CF-NP-6	82.98	3.53	6.81	6.68	**CF-VP-6**	85.18	5.98	---	8.84
CF-NP-7	82.90	3.59	6.80	6.71	**CF-VP-7**	84.99	6.09	---	8.92
G-NP-1	92.13	1.68	3.14	3.05	**G-VP-1**	93.05	2.94	---	4.01
G-NP-2	83.11	3.51	6.76	6.62	**G-VP-2**	85.33	5.91	---	8.76
G-NP-3	75.72	5.03	9.71	9.54	**G-VP-3**	79.03	8.34	---	12.63
G-NP-4	67.20	6.83	13.11	12.86	**G-VP-4**	71.59	11.39	---	17.02
G-NP-5	65.27	7.11	13.94	13.68	**G-VP-5**	69.87	11.95	---	18.18
G-NP-6	64.84	7.24	14.07	13.85	**G-VP-6**	69.55	12.12	---	18.33

Notes: the content of N in various CF-VP and G-VP catalysts exceeds the detection limits of the machine (Kratos AXIS Ultra spectrometer).

Table S5. Comparison of HER performance of CNT-VP with the recently reported metal-free catalysts in 0.5 M H_2SO_4.

Catalysts	Substrate	η@10 mA·cm^{-2} (mV)	Tafel slope (mV/dec)	Reference
CNT-VP	**GCE**	**41**	**36.5**	**This work**
**GDY/CFC*	GCE	94	45	*Angew. Chem. Int. Ed. 2022, 61, e202211094.*
Csp2-O-GDY	GCE	101	54	*2D Mater. 2022, 9, 024001.*
**COF-GO*	GCE	45	53	*Angew. Chem. Int. Ed. 2022, 61, e202113067.*
S doped G/CF	GCE	443	165	*ChemElectroChem 2022, 9, e202101455.*
G nanowall	GCE	320	86	*Appl. Surf. Sci. 2022, 592, 153327.*
Porous C Nanofiber	GCE	~260	96	*ACS Appl. Mater. Interfaces 2022, 14, 834.*
N, S codoped C	GCE	118.7	53	*Ionics 2022, 28, 1311.*
Edge-halogenated G	GCE	810	52	*Int. J. Hydrogen Energy 2022, 47, 15731.*
BCN/C_{60}	GCE	~210	87	*J. Am. Chem. Soc. 2021, 143, 1203.*
rGO/SiO_2	GCE	134	103	*Small Methods 2021, 5, 2100621.*
Ethylenediamine/CNT	GCE	~600	75	*New J. Chem. 2021, 45, 3932.*
Ionic liquid/CNT	GCE	135	38	*Nanoscale, 2021, 13, 4444.*
N doped vertical G	GCE	290	121	*Mater. Res. Bull. 2021, 134, 111094.*
1,2,4-triamino-GDY	GCE	82	74.13	*J. Catal. 2021, 395, 129.*
BCN@G	GCE	333	39	*ACS Appl. Energy Mater. 2021, 4, 3861.*
**GDY/CF*	GCE	68	41.6	*Small 2021, 17, 2006136.*
N doped C	GCE	151	45	*Polymers 2020, 12, 912.*
Black phosphorus/B doped G	GCE	385.9	110	*J. Mater. Chem. A 2020, 8, 20446.*
N, P codoped G	GCE	338	88	*J. Phys. Chem. C 2020, 124, 25701.*
O-SiBCN/rGO	GCE	590	127	*Sci. Rep. 2020, 10, 22003.*
Red P-rGO-g-C_3N_4	GCE	577	122.5	*Electrochim. Acta 2020, 338, 135851.*
N, S-CNT/ N, S-G	GCE	126	97	*J. Alloy. Compd. 2020, 848, 156528.*
N doped C	GCE	~730	---	*React. Chem. Eng. 2020, 5, 2134.*
P doped graphite	GCE	303	42	*Adv. Funct. Mater. 2020, 30, 1910741.*

N doped hollow C nanoflower	GCE	243	111	*Nanoscale 2020, 12, 14441.*
N, P, S tridoped porous C	GCE	260	86	*Carbon 2020, 162, 586.*
Red phosphorus nanoparticle	GCE	218	156	*Chem. Commun. 2020, 56, 2937.*
Red phosphorus/rGO/g-C_3N_4	GCE	575	122.5	*Electrochim. Acta 2020, 338, 135851.*
N doped C fiber	GCE	114.3	95.2	*Int. J. Hydrogen Energy 2020, 45, 4035.*
N-rich glassy C	GCE	190	55	*Mater. Res. Bull. 2020, 124, 110734.*
N doped porous C	GCE	179	98	*Nanomaterials. 2020, 10, 76.*
C_{60}-CNT	GCE	320	73.2	*J. Am. Chem. Soc. 2019, 141, 11658.*
N, P codoped G	GCE	106	67.3	*Energy Environ. Sci. 2019, 12, 2697.*
2D polyarylamines	GCE	424	99	*Chem. Eur. J. 2019, 25, 13860.*
**Dual graphitic-NG*	GCE	57	44.6	*Angew. Chem. Int. Ed. 2019, 58, 16973.*
N doped activated C	GCE	390	75.7	*Appl. Surf. Sci. 2019, 489, 725.*
CNT@N,P codoped C	GCE	167	81	*Nanoscale 2019, 11, 23027.*
**A-CFC*	CFC	78	37	*Nat. Commun. 2019, 10, 2281.*
N, S codoped CNT	GCE	131	71.9	*Chem. Commun. 2019, 55, 10011.*
Multiporous C	GCE	184	164	*New J. Chem. 2019, 43, 11653.*
N, P codoped G	GCE	340	118	*Adv. Sci. 2019, 6, 1900119.*
N doped CNT	GCE	360	118	*Catal. Lett. 2019, 149, 486.*
**N doped C*	GCE	90	43	*Energy Environ. Sci. 2019, 12, 322.*
N doped porous CF	GCE	248	135	*J. Solid State Chem. 2019, 274, 207.*
N doped C-CNT@poly (ethylene-alt-maleic acid)	N doped C	180	---	*Angew. Chem. Int. Ed. 2019, 58, 16217.*
3D NG sponge	GCE	267	69.7	*RSC Adv. 2019, 9, 99.*
3D G	Si substrate	107	64	*Angew. Chem. Int. Ed. 2018, 57, 192.*
C_3N_4@G	GCE	110	53	*ACS Catal. 2018, 8, 3965.*
N, S codoped G	GCE	230	72	*Angew. Chem. Int. Ed. 2018, 57, 13302.*
Hexagonal BN-G	GCE	~390	---	*Phys. Chem. Chem. Phys 2018, 20, 15007.*
NG	GCE	210	---	*ACS Energy Lett. 2018, 3, 1345.*
Ethylenediamine-functionalized multiwalled CNT	GCE	350	116	*Electrocatalysis 2018, 9, 573.*
P nanodot incorporated G	GCE	440	46	*J. Mater. Chem. A 2018, 6, 3141.*
NBC-ternary nanosheet	GCE	590	205	*Appl. Surf. Sci. 2018, 448, 618.*

N, P codoped G	GCE	~500	88	*ChemistrySelect 2018, 3, 6814.*
N functionalized CNT	GCE	250	---	*ChemCatChem 2018, 10, 3872.*
3D S doped G	GCE	218	64	*J. Mater. Sci. 2018, 53, 7767.*
Amine functionalized NG	GCE	350	113	*Carbon 2018, 138, 169.*
CN_x@NG	GCE	193	54	*ChemElectroChem 2017, 13, 2643.*
Graphite CN/B doped G	GCE	260	90	*Nanotechnology 2017, 29, 345705.*
g-C_3N_4@2D mesoporous G	GCE	219	53	*Adv. Funct. Mater. 2017, 27, 1606352.*
N doped C	GCE	276	94	*J. Mater. Chem. A 2017, 5, 6025.*
3D CNT	GCE	~300	---	*ACS Catal. 2017, 7, 2676.*
NG	GCE	128	66	*Appl. Catal. A: General 2017, 529, 127.*
S doped g-C_3N_4	GCE	186	84	*ACS Nano 2017, 11, 6004.*
NG	GCE	~380	---	*ChemCatChem 2017, 9, 4049.*
Covalent organic polymer	GCE	250	106	*ACS Catal. 2017, 7, 6120.*
NG	GCE	~380	---	*ChemCatChem 2017, 9, 4049.*
NSC	GCE	290	76.9	*ACS Nano 2017, 11, 7293.*
N, F codoped G	GCE	290	87	*Catal. Sci. Technol. 2017, 7, 2228.*
Pyrene-porphyrin-based crystalline covalent organic framework	GCE	380@5	116	*ACS Appl. Mater. Interfaces 2017, 9, 23843.*
N, S codoped G	Ni foam	298	75	*Int. J. Hydrogen Energy 2017, 42, 27004.*
***N doped CNT@NG*	GCE	62	50	*J. Mater. Chem. A 2017, 5, 6405.*
N doped C nanosheet	CC	320	198	*Int. J. Hydrogen Energy 2017, 42, 14390.*
Defect-rich, N, B codoped C nanocage	GCE	175.3	---	*Nano Energy 2017, 42, 334.*
G nanostripe	GCE	560	85.3	*Angew. Chem. Int. Ed. 2016, 55, 13965.*
N, P, S tridoped G	GCE	240	90	*Adv. Mater. 2016, 28, 10644.*
BC_7N_2	GCE	70@20	100	*Energy Environ. Sci. 2016, 9, 95.*
N, S codoped G	GCE	~300	120	*Nature Energy 2016, 1, 16130.*
Defect G	GCE	150	55	*Adv. Mater. 2016, 28, 9532.*
S-C_3N_4/CNT/CF	CF	236	81.6	*J. Mater. Chem. A 2016, 4, 12878.*
N, P codoped C network	GCE	163	89	*Angew. Chem. Int. Ed. 2016, 55, 2230.*
N, P codoped CF	GCE	151	69	*J. Mater. Chem. A 2016, 4, 13726.*

Plasma-etched N, S codoped G	GCE	149	78	*Electrochim. Acta 2016, 219, 781.*
S doped C_3N_4	GCE	145	51	*J. Mater. Chem. A 2016, 4, 12205.*
Horizontally-aligned CNT and G	GCE	420	121	*Carbon 2016, 107, 739.*
B, N codoped G	GCE	216	92	*J. Mater. Chem. A 2016, 4, 16469.*
Acid treated multiwalled CNT	GCE	~180	71.3	*ACS Appl. Mater. Interfaces 2016, 8, 35513.*
Plasma-etched S doped G	GCE	178	86	*Int. J. Hydrogen Energy 2016, 42, 4184.*
Defective activated C	GCE	334	66	*Chem. Commun. 2016, 52, 8156.*
N doped C nanosheet	GCE	137	131.6	*Electrochim. Acta 2016, 215, 223.*
N, S codoped CNT	GCE	~270	126	*Chem. Eur. J. 2016, 22, 10326.*
N, S codoped G	GCE	276	81	*Angew. Chem. Int. Ed. 2015, 54, 2131.*
NSC	GCE	120	67.8	*Nano Energy 2015, 16, 357.*
**C_3N_4@NG*	GCE	80	49.1	*ACS Nano 2015, 9, 931.*
N, P codoped G	GCE	213	79	*J. Mater. Chem. A 2015, 3, 12642.*
2D supramolecular polymer	GCE	333	80.5	*Angew. Chem. Int. Ed. 2015, 54, 12058.*
g-C_3N_4/N, P codoped G	GCE	340	90	*ChemCatChem 2015, 7, 3873.*
N, P codoped porous C	GCE	204	58.4	*J. Mater. Chem. A 2015, 3, 7210.*
Holey NG	GCE	340	99	*Nano Energy 2015, 15, 567.*
NSC	GCE	100	57.4	*J. Mater. Chem. A 2015, 3, 8840.*
N, P codoped G	GCE	~420	91	*ACS Nano 2014, 8, 5290.*
C_3N_4@NG	GCE	~240	51.5	*Nat. Commun. 2014, 5, 3783.*
B doped G	GCE	470	99	*Catal. Sci. Technol. 2014, 4, 2023.*
Activated CNT	GCE	220	71.3	*Chem. Commun. 2014, 50, 9340.*
g-C_3N_4 nanoribbon/G	GCE	207	54	*Angew. Chem. Int. Ed. 2014, 53, 13934.*
NG	GCE	240	109	*Sci. Rep. 2014, 4, 7557.*

Abbreviations: G = Graphene; rGO = Reduced graphene oxide; GCE = Glassy carbon electrode; CFC = Carbon fiber cloth; A-CFC = Amide group functionalized CFC; NG = N doped G; NSC = N, S codoped carbon; C = Carbon; CC = Carbon cloth; CF = Carbon fiber; g-C_3N_4 = graphitic-C_3N_4; CNT = Carbon nanotube; C_{60} = Buckminsterfullerene; GDY = Graphdiyne; COF = covalentorganic framework

Notes: the ***** prefix indicates that the overpotential and Tafel slope of the catalysts are included in **Fig. 3c**.

Table S6. Parameters obtained by fitting the Nyquist plots of CNT-V, CNT-N, CNT-P, CNT-NP and CNT-VP using the equivalent circuit in ***Fig. S21***.

Samples	R_s (Ω)	R_1 (Ω)	CPE1 (F)	R_{ct} (Ω)	CPE2 (F)
CNT-V	2.17	0.41	4.25×10^{-12}	65.69	2.45×10^{-7}
CNT-N	2.14	0.35	4.98×10^{-12}	60.53	2.66×10^{-7}
CNT-P	2.11	0.32	5.45×10^{-12}	52.18	3.08×10^{-7}
CNT-NP	2.07	0.24	7.27×10^{-12}	34.61	4.65×10^{-7}
CNT-VP	2.01	0.19	9.18×10^{-12}	21.59	7.45×10^{-7}

Table S7. The detailed dosages of melamine and phosphoric acid in the synthesis of various CNT-NP catalysts.

Samples	Melamine (mg)	Phosphoric acid (mL)
CNT-NP	60	0.15
CNT-NP-1	80	0.10
CNT-NP-2	40	0.20
CNT-NP-3	20	0.05
CNT-NP-4	40	0.10
CNT-NP-5	80	0.20
CNT-NP-6	100	0.25
CNT-NP-7	120	0.30
CNT-NP-8	140	0.35

Table S8. The detailed dosages of melamine and phosphoric acid in the synthesis of various CF-NP and G-NP, respectively.

Samples	Melamine (mg)	Phosphoric acid (mL)
CF-NP-1	20	0.05
CF-NP-2	40	0.10
CF-NP-3	60	0.15
CF-NP-4	80	0.20
CF-NP-5	100	0.25
CF-NP-6	120	0.30
CF-NP-7	140	0.35
G-NP-1	20	0.05
G-NP-2	40	0.10
G-NP-3	60	0.15
G-NP-4	80	0.20
G-NP-5	100	0.25
G-NP-6	120	0.30